ELSEVIER

Chemical Engineering Journal 93 (2003) 3–9

Chemical Engineering Journal

www.elsevier.com/locate/cej

Selective oxidation of methane in an SOFC-type reactor: effect of applied potential

Tomohiko Tagawa [a,*], Koujiro Kuroyanagi [a], Shigeo Goto [a], Suttichai Assabumrungrat [b], Piyasan Praserthdam [b]

[a] *Department of Chemical Engineering, Nagoya University, Chikusa, Nagoya 464-8603, Japan*
[b] *Department of Chemical Engineering, Research Center on Catalysis and Catalytic Reaction Engineering, Chulalongkorn University, Bangkok 10330, Thailand*

Abstract

The effect of applied potential on the selective oxidation of methane in a solid oxide fuel cell (SOFC)-type reactor was investigated. A tube-type YSZ was used as an electrolyte where a $La_{1.8}Al_{0.2}O_3$ anode and a conventional $La_{0.85}Sr_{0.15}MnO_3$ cathode were deposited on the inner and outer surfaces of the tube, respectively. The fuel cell-type temperature-programmed desorption (FC-TPD) measurements revealed that the amount of adsorbed oxygen on the anode catalyst was altered with the applied potential. Increasing the applied potential increased the amount of weakly adsorbed oxygen at the "oxygenate site". Two operating modes of the SOFC-type reactor were carried out. In the normal mode, it was found that the rate of C_2 formation was not affected by an applied potential. The positive potential increased the rate of carbon oxides formation, especially the product CO, while the negative potential suppressed the rates of CO and CO_2 formation. For the mixed-flow mode, even though the electrochemically promoted rates did not show significant improvement over the open-circuit rates, the catalytic activities of the anode catalyst to different products were altered by the applied potential with non-Faradaic manner. The change in the selectivity of the active site gave a new aspect to non-Faradaic electrochemical modification of catalytic activity (NEMCA) phenomena.

Keywords: Solid oxide fuel cell; Oxidative coupling of methane; Temperature-programmed desorption; NEMCA

1. Introduction

The effective utilization of methane as chemical resources has been strongly desired. Oxidative coupling of methane is an attractive process for producing C_2 compounds (ethane and ethene) and many studies have been done in this field since Keller and Bhasin [1] firstly demonstrated this possibility. However, a deep oxidation reaction seems to be a more favorable route. A key in achieving high C_2 compounds was to control type and state of oxygen species [2]. Several researchers have tested a number of alternatives including: (a) using a sequential feed of oxygen and methane, (b) using a metal oxide in which lattice oxygen was the reactant instead of gaseous oxygen, and (c) using a solid electrolyte fuel cell reactor. Electrochemically permeated oxygen showed higher activity and selectivity for the production of C_2 compounds compared to surface oxygen from gas phase [3]. A number of reviews were published on this topic [4–8].

In our previous papers, a solid oxide fuel cell (SOFC)-type reactor for a chemicals energy co-generation was investigated [9–13]. In the reactor, the cathode activated gaseous oxygen into O^{2-} species, which permeated through a solid electrolyte. A selective oxidation catalyst was used as an anode where methane was selectively oxidized into valuable C_2 products with permeated oxygen species. The design strategy of an anode catalyst for the SOFC-type reactor was proposed where TPD technique played an important role [11]. Because this system was used as a membrane reactor, gaseous oxygen was not directly mixed with methane. It improved safety of the reaction mixture and avoided gaseous combustion reaction. Moreover, when air was used as an oxidant, no nitrogen accumulates in the reaction zone, since only oxygen was selectively permeated through YSZ. The reactor also provided direct conversion of chemical energy to electricity with high efficiency during the selective oxidation.

In the fuel cell-type reactor, it is also important to control the activity of surface oxygen species on the anode catalyst by applying external potential to the electrode catalysts so that partial oxidation reactions can be enhanced by many orders of magnitude. These phenomena were often referred as the electrochemical promotion (EP) or non-Faradaic electrochemical modification of catalytic activity (NEMCA) effect

* Corresponding author.
E-mail address: tagawa@nuce.nagoya-u.ac.jp (T. Tagawa).

1385-8947/02/$ – see front matter
PII: S1385-8947(02)00105-5

Nomenclature

E	applied potential (V)
I	current (mA)
r_i	rate of formation of species i (mol/s m^2-YSZ)
ΔT	rate of temperature increase (K/s)

Greek symbols

Λ_i	rate enhancement factor of product i (–)
ρ_i	rate improvement factor of product i (%)

[14]. It has been extensively applied to more than 50 catalytic reactions on Pt, Pd, Rh, Ag, Ni, Au, IrO_2, and RuO_2 surfaces [15].

In this study, the effect of applied potential to the selective oxidation of methane in the SOFC-type reactor was studied. The reactor was operated under both normal fuel cell mode and mixed-flow mode in which the NEMCA effect can take place. A fuel cell-type temperature-programmed desorption (FC-TPD) technique was developed to investigate the effect of applied potential on nature of adsorbed oxygen.

2. Experimental

2.1. SOFC-type reactor

The schematic diagram of the SOFC-type reactor is illustrated in Fig. 1. A tube-type YSZ membrane (8 mol% Y_2O_3, thickness = 1.5 mm, inside diameter = 18 mm, outside diameter = 21 mm, length = 500 mm) was used as an electrolyte. $La_{1.8}Al_{0.2}O_3$ (abbreviated as LaAlO) prepared by a mist decomposition method was deposited as an anode catalyst on the inner surface of the tube while a conventional cathode material of $La_{0.85}Sr_{0.15}MnO_3$ (abbreviated as LSM) was prepared on the outer side. Details of the preparation methods for the above electrodes and other anode materials of CeAlO and Ni cermet were described elsewhere [11–13,16]. Platinum wires were connected to platinum meshes placed on both electrode surfaces to serve as current collectors. The outlet gas from the anode side was directly connected to a gas chromatography for analysis of products. A potentiostat was used to supply an external potential to the electrodes. Current and electromotive force can be measured using a multimeter under closed- and open-circuit conditions, respectively.

Two modes of operation were carried out in the SOFC-type reactor. The first one was a normal mode in which the reactants (methane and oxygen) were introduced separately to the anode and cathode sides, respectively. The reaction was conducted with permeated oxygen species. The latter one was a mixed-flow mode in which oxygen in air was co-fed with methane to the anode side. The SOFC-type reactor can be applied with either positive or negative potential during the operation. Oxygen transport from the cathode side to the anode side was promoted under the applied positive potential. Negative potential was carefully applied so that the current (i.e. permeation of oxygen) did not approach a negative value. Table 1 summarizes the standard operating conditions of the SOFC-type reactor.

Table 1
Standard operating conditions of the SOFC-type reactor

Parameters	Values
Temperature (K)	1223
Applied potential (V)	0
Pressure (kPa)	101.3
Flow rate for normal fuel cell mode	
Cathode side: O_2 (mol/s)	6.8×10^{-6}
Anode side: CH_4 (mol/s)	6.8×10^{-6}
Flow rate for mixed-flow fuel cell mode	
Cathode side: O_2 (mol/s)	6.8×10^{-6}
Anode side: CH_4 (mol/s)	51.0×10^{-6}
O_2 (mol/s)	2.4×10^{-6}
N_2 (mol/s)	48.6×10^{-6}
YSZ surface area (m^2)	1.6×10^{-2}

2.2. Temperature-programmed desorption (TPD)

2.2.1. Conventional TPD

In the conventional TPD measurement, a constant amount of powder sample of 0.58 g was packed into a quartz tube (8 mm o.d., 6 mm i.d.). After pretreatment by purging air at 983 K for 16 h, the temperature was lowered to 323 K and kept constant for 0.5 h in the air stream. After helium gas (1.36×10^{-5} mol/s) was passed through the tube for 0.5 h, the temperature was increased at a desired rate (ΔT). The exit gas was continuously monitored by a thermal conductivity cell.

2.2.2. Fuel cell-type temperature-programmed desorption measurement

There were two types of experimental set-ups for FC-TPD measurement according to the configuration of YSZ electrolytes, i.e. plate and tube. The experimental set-up for the FC-TPD measurement of the tube-type YSZ was similar to the SOFC-type reactor shown in Fig. 1. Instead of CH_4, He as a carrier gas was fed to the anode side and the outlet was directly connected to a thermal conductivity detector. For the plate-type YSZ, the electrodes were prepared on a YSZ plate (8 mol% Y_2O_3, thickness = 0.3 mm, diameter = 42 mm) using the same preparation procedure as the tube YSZ. The cell was fabricated between two ceramic tubes with Pyrex seals. The experimental set-up was similar to that reported previously [11]. The experimental procedures for both configurations were the same: helium (1.36×10^{-5} mol/s) and oxygen (1.02×10^{-5} mol/s) were fed to the anode and cathode sides, respectively. The FC-TPD measurement was divided into two modes, i.e. open-circuit

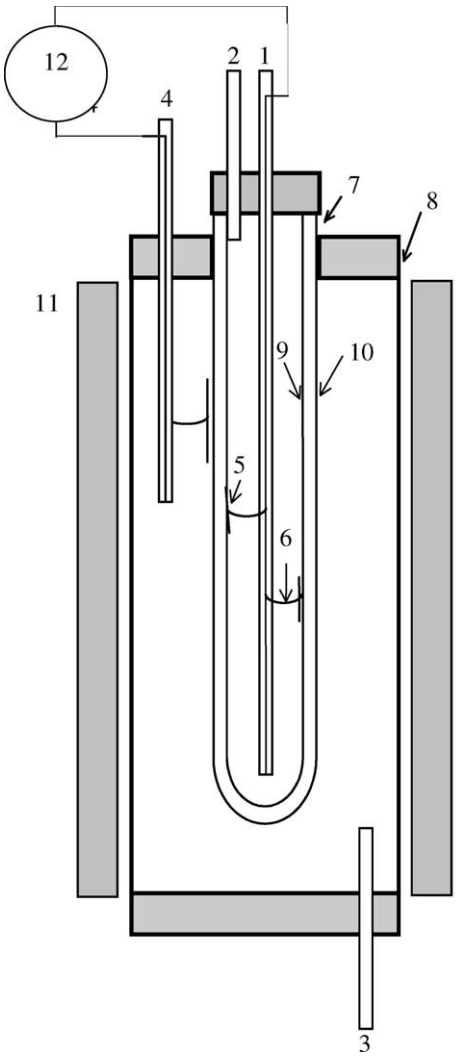

1. Anode side feed (CH_4)
2. Exit gas from anode side
3. Cathode side feed (O_2)
4. Exit from cathode side
5. Platinum mesh
6. Platinum wire
7. YSZ tube
8. Quartz tube
9. Anode (LaAlO)
10. Cathode (LSM)
11. Furnace
12. Ammeter/Voltmeter/Potentiostat

Fig. 1. Schematic diagram of the SOFC-type reactor.

and closed-circuit modes. Both electrodes were disconnected in the open-circuit mode and the system behaved like the conventional TPD. For the closed-circuit mode, both electrodes were connected to allow oxygen permeation from the cathode to the anode side.

The pretreatment was carried out under flows of air (1.36×10^{-5} mol/s) on the anode and oxygen (1.02×10^{-5} mol/s) on the cathode for 7 h at 1273 K. For the open-circuit FC-TPD, four values of applied potential, i.e. $E = -1$, 0, 1 and 2 V, were employed by the potentiostat during the pretreatment in order to investigate the effect of applied potential on the nature of adsorbed oxygen on the anode catalyst. For the closed-circuit FC-TPD, the system was pretreated at the same condition but the applied potential was not charged ($E = 0$ V) during the pretreatment.

After the pretreatment, the temperature was lowered to 873 K for the plate-type set-up and to 600 K for the tube-type set-up under the same gas flow as the pretreatment. Anode gas was then changed to carrier gas flow (He: 1.36×10^{-5} mol/s) while cathode gas was not changed (O_2: 1.02×10^{-5} mol/s). After the baseline was stabilized, the FC-TPD measurement was started at a desired rate (ΔT) with various levels of potential applied to the cell.

3. Results and discussion

3.1. TPD measurement

The conventional TPD measurements of powder samples of the anode catalyst (LaAlO) and the electrolyte (ZrO_2) were carried out to illustrate the nature of adsorbed oxygen. From Fig. 2, the TPD spectra of LaAlO showed two oxygen peaks at temperature below 1200 K. In our previous works, the oxygen desorption at high temperature (above 1200 K) was lattice oxygen while the two peaks at the lower temperature indicated surface oxygen species. The oxygen species at low temperature were active for CO and CO_2 formation

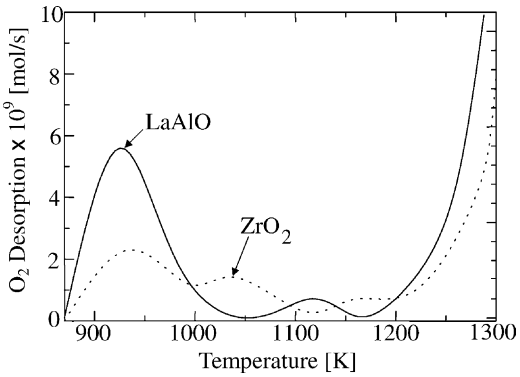

Fig. 2. Powder TPD results of LaAlO and ZrO_2 ($\Delta T = 0.133$ K/s).

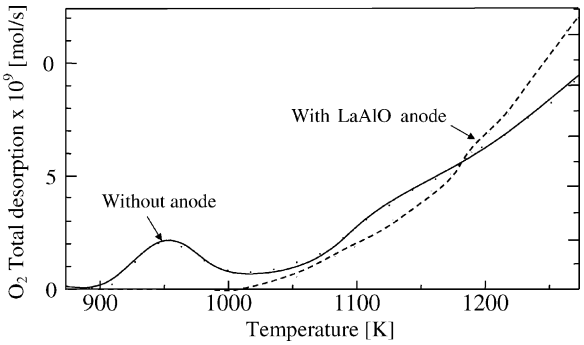

Fig. 3. Effect of anode catalyst on FC-TPD results (plate-type YSZ, closed circuit, $\Delta T = 0.033$ K/s).

while the oxygen species at higher temperature were active for oxidative coupling. These were represented as "oxygenate site" and "coupling site", respectively [11]. The TPD spectra of ZrO_2 indicated that lattice oxygen of ZrO_2 can be supplied to the anode above 1100 K with a considerable amount of adsorbed oxygen at 925 K.

FC-TPD measurements were then conducted. Figs. 3 and 4 represent results for the plate system, while Figs. 5 and 6 represent results for the tubular system. It should be noted that the open-circuit FC-TPD mode behaved similar to the

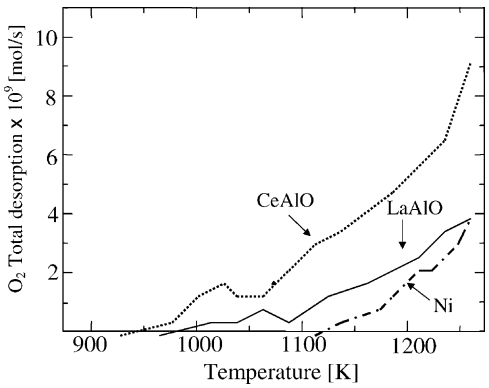

Fig. 4. Effect of anode catalysts on FC-TPD results (plate-type YSZ, closed circuit, $\Delta T = 0.033$ K/s).

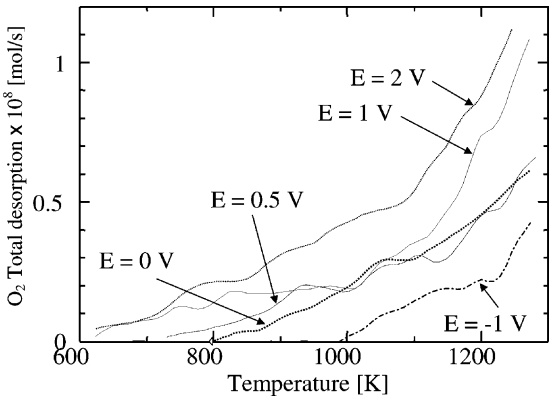

Fig. 5. Effect of applied potential on closed-circuit FC-TPD results (tube-type YSZ, $\Delta T = 0.083$ K/s).

conventional TPD. Because the circuit was not connected, there was no oxygen permeation from the cathode side to the anode side. The observed O_2 in the anode side corresponded to the desorbed oxygen from the anode and the electrolyte (Fig. 6). On the other hand, the closed-circuit FC-TPD mode provided the combined effect of oxygen desorption and oxygen permeation through the electrolyte. Therefore, the observed oxygen during TPD was represented as "O_2 total desorption" in Figs. 3–5. If the active oxygen desorbed from anode was not supplied by permeation, only a desorption peak should be observed at the corresponding temperature to powder TPD. On the other hand, if it is supplied by permeation, a continuous release of oxygen should be observed. In this case, the rate will be determined by either the desorption rate or the permeation rate depending on the temperature.

Fig. 3 shows the closed-circuit FC-TPD results of the plate configuration when the cell was prepared with and without LaAlO anode. It was observed that oxygen was electrochemically permeated through the cell and lattice oxygen can be supplied from the electrolyte to the anode. It should be noted that at $T > 1200$ K, O_2 permeated became higher with LaAlO anode than without anode. This is because the

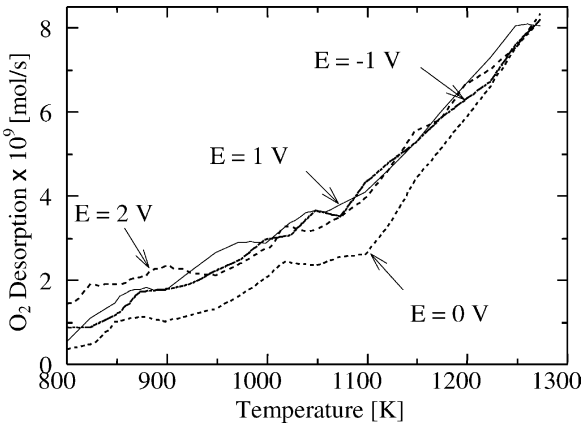

Fig. 6. Effect of pretreatment condition on open-circuit FC-TPD results (tube-type YSZ, $\Delta T = 0.083$ K/s).

anode catalyst played an important role on facilitating the electrochemical conversion of lattice oxygen to molecular oxygen. Fig. 4 shows FC-TPD results of other anode catalysts of CeAlO and Ni. It was indicated that the types of anode catalyst played an important role on the oxygen permeation. These results show that the permeated lattice oxygen was once activated on anode catalyst and then desorbed. Thus, the selection of anode is quite important for the design of SOFC-type reactor. In the following studies, LaAlO was selected as an anode catalyst due to its high selectivity to oxidative coupling of methane [11].

The effect of applied potential was investigated using both closed-circuit and open-circuit FC-TPD techniques. Fig. 5 shows closed-circuit FC-TPD results at $E = -1$, 0, 0.5, 1 and 2 V. It was observed that oxygen was preferentially transported to the anode side at high temperature and applied potential. It should be noted that oxygen species at "oxygenate site" (800–1000 K) were enhanced by positive potential. In spite that the negative potential decreased these "oxygenate" species. Fig. 6 shows the open-circuit FC-TPD results after the system was pretreated under the applied potential, $E = -1$, 0, 1 and 2 V during the oxygen adsorption stage. In this open-circuit, FC-TPD results excluded the effect of oxygen permeation. On the other words, only adsorbed oxygen was detected. It was found that by applying positive potential to the electrode catalysts during the adsorption stage, the amount of adsorbed oxygen increased, particularly the surface oxygen. The applied potential did not alter the nature of lattice oxygen since the amount of lattice oxygen desorption from different pretreatment was almost the same. The increased amount of oxygen adsorption due to the applied potential was also reported in another system in which electrochemical O^{2-} was pumped to Pt and Ag catalyst on YSZ [17]. The presence of pre-adsorbed oxygen caused back-spillover of large amounts of oxygen on the catalyst surface and led to the formation of two oxygen adsorption states [17].

With negative applied potential, oxygen adsorption was also enhanced. During the pretreatment with negative potential of −1 V, the negative current was observed. This suggested that oxygen in air at the anode catalyst side was transported toward pure oxygen side through YSZ. As a result, oxygen was accumulated on the anode catalyst from the gas phase and this may cause the increase of the amount of adsorbed oxygen on the anode catalyst.

3.2. SOFC-type reactor studies

3.2.1. Normal mode

Fig. 7 shows the rates of formation (r_i) of the products, i.e. C_2 compounds (i.e. ethane and ethene), CO and CO_2, as a function of positive applied potential under the normal mode of operation. Without the applied potential, $E = 0$ V, the C_2 compounds were formed selectively. When the positive potential was supplied to the cell to enhance the oxygen transportation, the rate of formation of carbon oxides

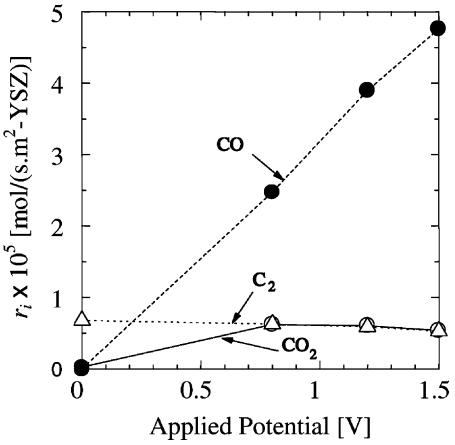

Fig. 7. Effect of applied positive potential on normal fuel cell operation ($T = 1223$ K).

increased, particularly CO. However, no significant change was observed on C_2 formation. These results corresponded well with the closed-circuit FC-TPD results in which the applied potential increased the amount of oxygen at the "oxygenate site" while it did not significantly affect the lattice oxygen. When the negative potential was applied, the rates of formation of CO and CO_2 were suppressed while that of C_2 remained constant as shown in Fig. 8. This also agreed with the FC-TPD results with negative potential shown in Fig. 5. These behaviors were probably caused by the selective influence of electrochemical oxygen pumping on the nature of the active sites on the anode catalyst. In this case, the applied potential influenced the oxygen transport to the LaAlO anode at the specific site. Thus, the nature of the catalyst greatly influenced by applied potential.

Among the reported results, no influence of the rate of the electrochemical oxygen pumping (i.e. applied positive potential) on the activity of the catalyst was observed on pure Ag [3] whereas in the Li/MgO–Ag system, the activity of the catalyst decreased [18]. For the Bi_2O_3–Ag system, an increase in the activity and selectivity was observed with increased rates of oxygen pumping [3].

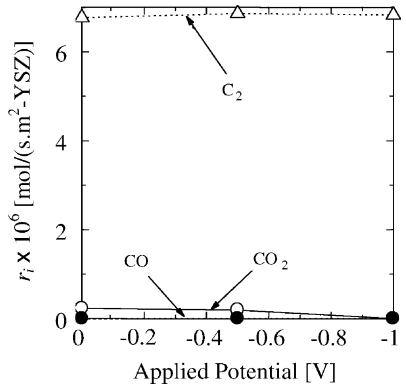

Fig. 8. Effect of applied negative potential on normal fuel cell operation ($T = 1223$ K).

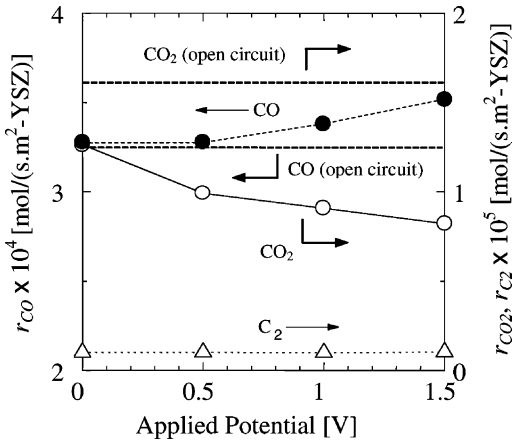

Fig. 9. Effect of applied positive potential on mixed-flow fuel cell operation ($T = 1223$ K).

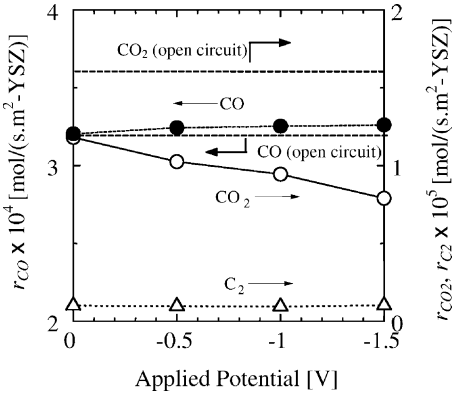

Fig. 10. Effect of applied negative potential on mixed-flow fuel cell operation ($T = 1223$ K).

3.2.2. *Mixed-flow mode*

In the mixed-flow mode, oxygen was co-fed with methane to the anode side. Figs. 9 and 10 show the rates of formation of the products as a function of applied positive and negative potentials, respectively. The dashed lines represent the results from the open-circuit operation, which behaved as an ordinary flow-type reactor. It was found that when the circuit was closed with no external applied potential, the rate of formation of CO_2 was significantly decreased while those of CO and C_2 (not shown) were almost the same. Table 2 provides more information of the results on the amount of Faradaic oxygen (electrochemically permeated oxygen) calculated from the corresponding current, the amount of reacted oxygen and the rate of methane consumption ($-r_{CH_4}$). The data in Tables 2 and 3 show the two types of parameters derived from the experimental results to describe the NEMCA effect, i.e. rate improvement factors (ρ_i) and Faradaic enhancement factor (Λ_i) which were defined as follows:

$$\rho_i = \frac{r_i - r_{i,\text{open}}}{r_{i,\text{open}}} \times 100\% \quad (1)$$

$$\Lambda_i = \left| \frac{r_i - r_{i,\text{open}}}{\text{Faradaic oxygen}} \right| \quad (2)$$

where $r_{i,\text{open}}$ is an open-circuit rate of formation of product i (corresponding to the rate of normal gas-phase catalytic oxidation). The first parameter represented the change of the rate of formation of product i from the open-circuit rate when an external potential was applied, while the latter parameter showed the change of reaction rate of product i compared to the Faradaic oxygen which was electrochemically supplied to the reaction chamber. It was found that when positive potential was applied, the rate improvement factor of CO formation increased while that of CO_2 decreased. The negative potential also influenced the performance in the similar manner. However, it was observed that the applied potential scarcely affected the rate of C_2 formation. When considering the rates of reacted oxygen and methane

Table 3
Summary of NEMCA effect

Applied potential (V)	ρ_i (%)			Λ_i (–)		
	CO	CO_2	C_2	CO	CO_2	C_2
Open	0	0	0	–	–	–
−1.5	1.8	−23.2	2.2	9.8×10^2	6.7×10^2	4
−1.0	4.0	−14.0	−5.4	1.0×10^4	1.8×10^3	42
−0.5	1.2	−9.2	0.0	71	28	0
0	0.5	−24.7	0.0	21	53	0
0.5	2.2	−41.0	1.5	8	8	0
1	5.5	−46.0	−0.6	8	3	0
1.5	9.8	−51.1	2.8	6	2	0

Table 2
Summary of results from the mixed-flow SOFC

Applied potential (V)	I (mA)	Faradaic O (mol/(s m^2-YSZ))	Reacted O (mol/(s m^2-YSZ))	$-r_{CH_4}$ (mol/(s m^2-YSZ))
Open	0	0	1.03×10^{-3}	3.39×10^{-4}
−1.5	−0.018	-5.82×10^{-9}	1.03×10^{-3}	3.41×10^{-4}
−1.0	0.004	1.16×10^{-9}	1.06×10^{-3}	3.50×10^{-4}
−0.5	0.170	5.50×10^{-8}	1.04×10^{-3}	3.42×10^{-4}
0	0.240	7.76×10^{-8}	1.03×10^{-3}	3.37×10^{-4}
0.5	2.63	8.51×10^{-7}	1.02×10^{-3}	3.40×10^{-4}
1	7.00	2.26×10^{-6}	1.05×10^{-3}	3.49×10^{-4}
1.5	15.20	4.92×10^{-6}	1.09×10^{-3}	3.62×10^{-4}

shown in Table 2, it was clear that the electrochemically promoted overall catalytic rates did not show significant enhancement over the open-circuit catalytic rate as reported in many NEMCA studies [19]. The reason of low enhancement may be due to the high operating temperature ($T = 1223\,K$) where the catalytic activity was already high. However, the change in the selectivity of the active site due to the electrochemical modification gave a new aspect to the NEMCA phenomena. The change in rate of formation of the product can be as large as 10^4 times higher than the electrochemically supplied oxygen, showing the electrochemical modification of selectivity by non-Faradaic manner. More detailed studies are underway on these observations.

4. Conclusion

The effect of applied potential on the performance of the selective oxidation of methane in a $La_{0.85}Sr_{0.15}MnO_3$/YSZ/$La_{1.8}Al_{0.2}O_3$ SOFC-type reactor was studied. The FC-TPD measurements revealed that the amount of adsorbed oxygen on the anode catalyst was altered with the applied potential. Increasing the applied potential increased the amount of weakly adsorbed oxygen at the "oxygenate site". Two operating modes of the SOFC-type reactor were carried out. In the normal mode, it was found that the rate of C_2 formation was not affected by an applied potential. The positive potential increased the rate of CO formation, while the negative potential suppressed the rates of CO and CO_2 formation. For the mixed-flow mode, even though the electrochemically promoted rate did not show significant improvement over the open-circuit rate, the catalytic activities of the anode catalyst to different products (selectivity) were altered by the applied potential with non-Faradaic manner. The change in the selectivity of the active site gives a new aspect to NEMCA phenomena.

Acknowledgements

A part of this study was supported by Monbukagakusho-Grant-in-aid for Scientific Research, Priority area (B) 754, No. 13126211. The support from TJTTP-OECF is also gratefully acknowledged.

References

[1] G.E. Keller, M.M. Bhasin, J. Catal. 73 (1982) 9.
[2] E.E. Wolf, Methane Conversion by Oxidative Process, Van Nostrand Reinhold, New York, 1992.
[3] K. Otsuka, S. Yokoyama, A. Morikawa, Chem. Lett. (1985) 319–322.
[4] G.J. Hutchings, M.S. Scurrell, J.R. Woodhouse, Chem. Soc. Rev. 81 (1989) 251–283.
[5] Y. Amenomiya, V.I. Birss, M. Goledzinowski, J. Galuszka, A.R. Sanger, Catal. Rev. Sci. Eng. 32 (1990) 163–227.
[6] D. Eng, M. Stoukides, Catal. Rev. Sci. Eng. 33 (1991) 375–412.
[7] E.N. Voskresenskaya, V.G. Roguleva, A.G. Anshits, Catal. Rev. Sci. Eng. 37 (1995) 101–143.
[8] M. Stoukides, Catal. Rev. Sci. Eng. 42 (2000) 1–70.
[9] T. Tagawa, K.K. Moe, M. Ito, S. Goto, Chem. Eng. Sci. 54 (1999) 1553–1557.
[10] T. Tagawa, H. Imai, J. Chem. Soc., Faraday Trans 84 (1) (1988) 923–929.
[11] T. Tagawa, K.K. Moe, T. Hiramatsu, S. Goto, Solid State Ionics 106 (1998) 227–235.
[12] K.K. Moe, T. Tagawa, S. Goto, J. Ceram. Soc. Jpn. 106 (1998) 242–247.
[13] K.K. Moe, T. Tagawa, S. Goto, J. Ceram. Soc. Jpn. 106 (1998) 754–758.
[14] C.G. Vayenas, S. Bebelis, S. Neophytides, J. Phys. Chem. 92 (1998) 5083–5085.
[15] A.D. Frantzis, S. Belelis, C.G. Vayenas, Solid State Ionics 136–137 (2000) 863–872.
[16] A.S. Carrillo, T. Tagawa, S. Goto, Mater. Res. Bull. 36 (2001) 1017–1027.
[17] D. Tsiplakides, S. Neophytides, C.G. Vayenas, Solid State Ionics 136–137 (2000) 839–847.
[18] S. Seimanides, M. Stoukides, J. Electrochem. Soc. 133 (1986) 1535.
[19] C.G. Vanenas, S. Bebelis, Catal. Today 51 (1999) 581–594.